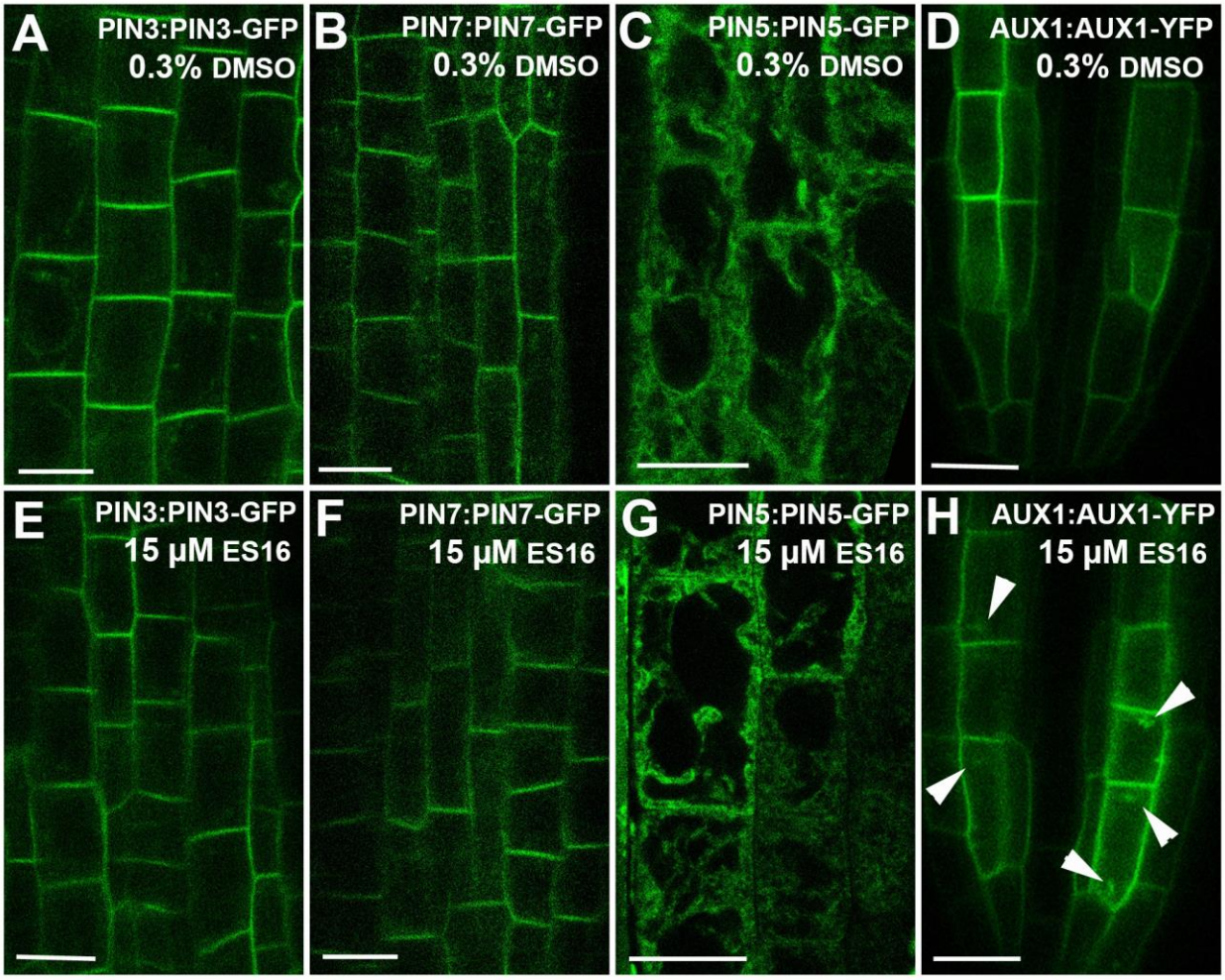

Supplemental Figure 1. ES16 does not interfere with PIN3, PIN7 and PIN5 but induces aggregates of AUX1.

(A to D) Subcellular localization of PIN3 (A), PIN7 (B), PIN5 (C) and AUX1 (D) after treatment with 0.3% DMSO. (E to H) Subcellular localization of PIN3 (E), PIN7 (F), PIN5 (G) and AUX1 (H) after treatment with 15 µM ES16. ES16 does not interfere with basally localized PIN3, PIN7 and ER localized PIN5, but induces aggregates in AUX1. White arrowheads in H represent ES16-induced aggregates. Representative images are shown. Scale bars, 10 µm.

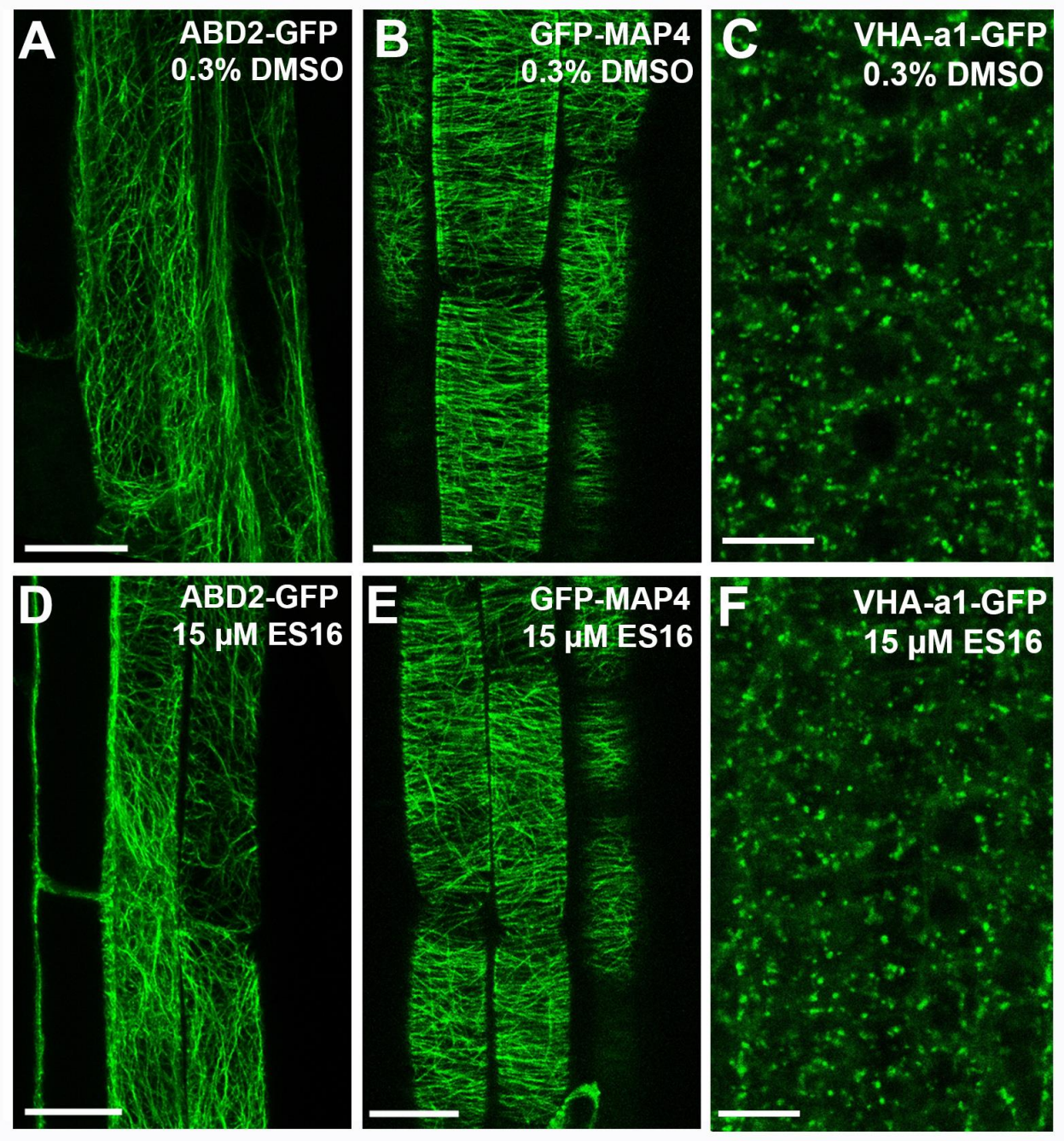

Supplemental Figure 2. ES16 does not affect VHA-a1 or cytoskeleton organization.

(A to C) Images of F-actin labeled by ABD2-GFP (A), tubulin marker GFP-MAP4 (B) and TGN localized VHAa1 (C) after DMSO treatment. (D to F) ES16 treatment does not affect the organization of actin (D) or TUBULIN (E) or alter the subcellular localization of VHAa1 (F). Representative images are shown. Scale bars, 10 μm.

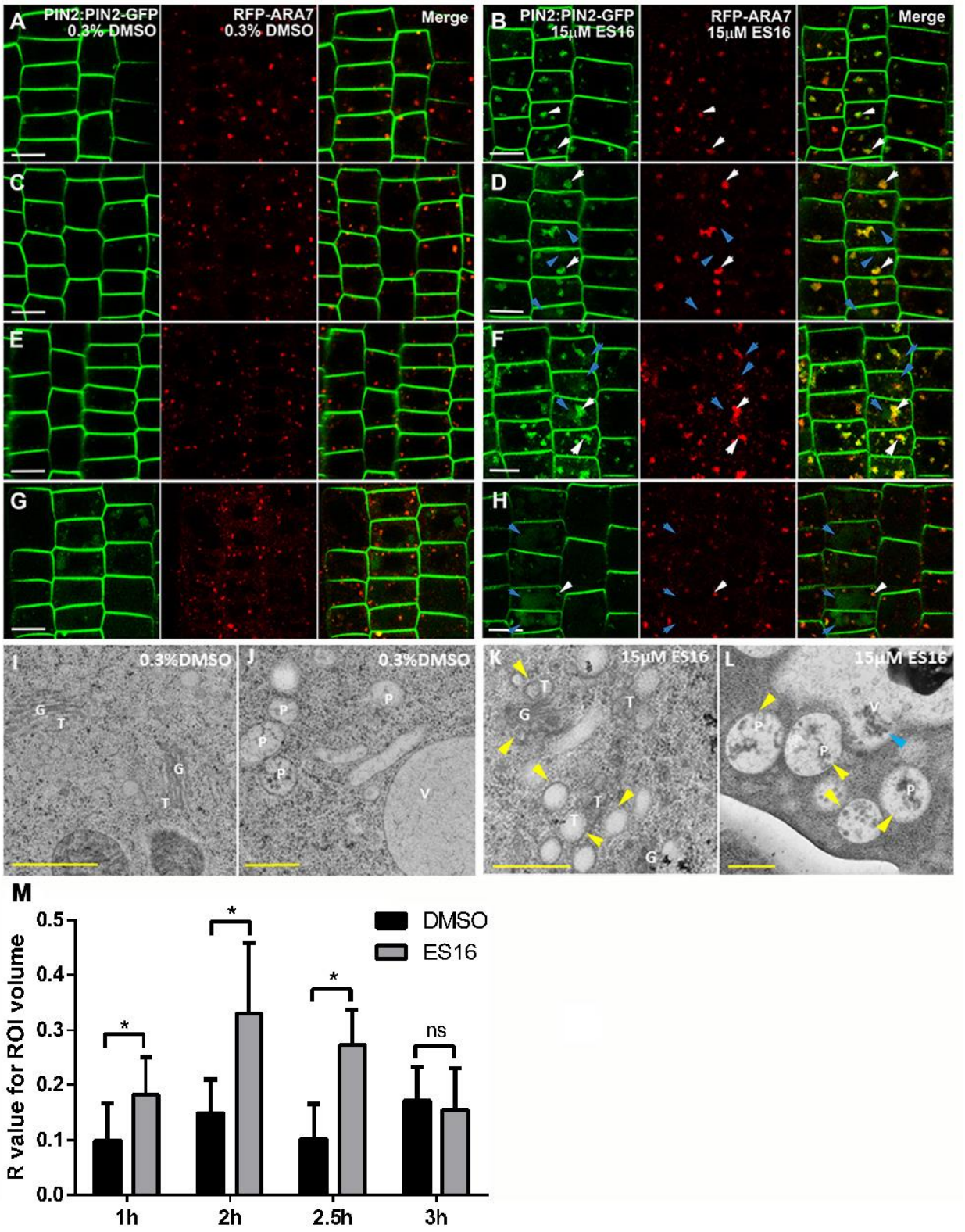
A
PIN2:PIN2-GFP
0.3% DMSO
RFP-ARA7
0.3% DMSO
Merge
B
PIN2:PIN2-GFP
15μM ES16
RFP-ARA7
15μM ES16
Merge
C
D
E
F
G
H
I
0.3%DMSO
G
T
G
T
J
0.3%DMSO
P
P
P
P
V
K
15μM ES16
T
T
G
T
T
G
L
15μM ES16
V
P
P
P
M
R value for ROI volume
0.5
0.4
0.3
0.2
0.1
0.0
DMSO
ES16
*
*
*
ns
1h
2h
2.5h
3h

Supplemental Figure 3. ES16 promotes vacuole transport via the transition through PVC.

(A to D) ES16 induced colocalization between PIN2 aggregates and enlarged ARA7 from 1 h to 2 h treatment (B and D compared with A and C; white arrowheads indicate colocalization between the two vesicle populations). Starting from 2 h, partial vacuole localization of PIN2 could be detected in ES16-treated sample but not in the control samples (blue arrowheads in D). (E to H) Long-term treatment with ES16 resulted in less colocalization of PIN2 with ARA7 with more PIN2 transferred to the vacuole and reduced size and signal intensity of ARA7 (blue arrowheads represent vacuole localization of PIN2, which are not co-localized with ARA7). (I to L) Transmission electron microscopy (TEM) results of cells in root tip sections after DMSO (I and J) or ES16 (K and L) treatment. ES16 induced vacuolization of vesicles budding from the TGN and some of the enlarged TGN were detached from Golgi (K, yellow arrowheads). ES16 also induced PVC clusters not exhibiting fusion with vacuole (L, yellow arrowhead). G, Golgi; T, trans-Golgi network (TGN); P, prevacuolar compartment (PVC). (M) Quantification of colocalization of PIN2 and ARA7. Analysis was performed using the Imaris co-localization software module function. Thresholds were set automatically and Pearson correlation coefficient for the ROI volume was calculated automatically. Error bars represent SD of nine independent samples each. Representative images are shown. Scale bars, 10 μm (A to H); 500 nm (I to L).

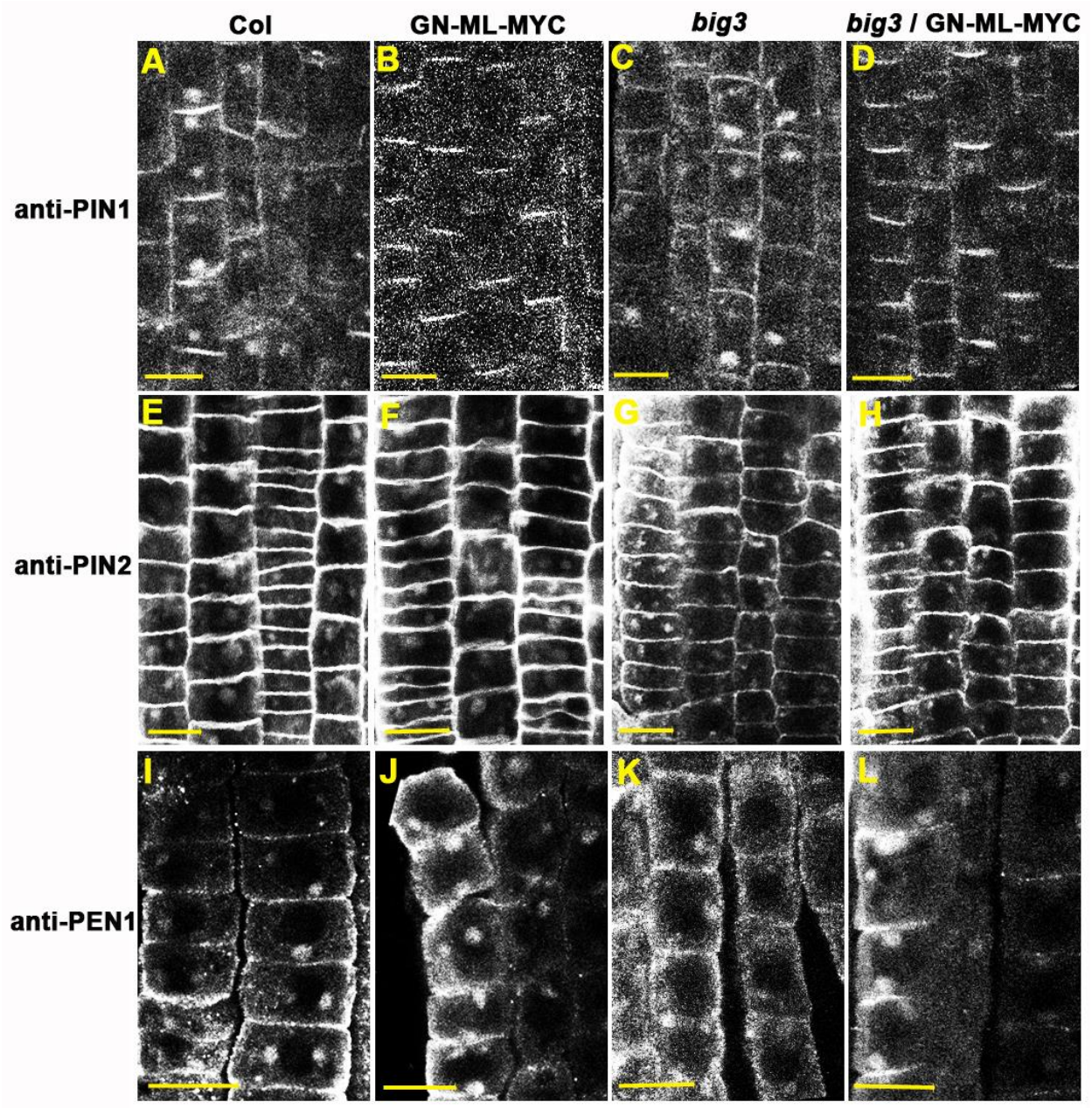

Supplemental Figure 4. BIG clade ARF-GEFs regulate non-basal trafficking.

(A to D) Immunostaining of PIN1 in Col (A), GN-ML-MYC(B), *big3* (C) and *big3* / GN-ML-MYC (D) mutants after 1 h treatment with 50 µM BFA. (E to H) Immuno-localization of PIN2 in Col (E), GN-ML-MYC (F), *big3* (G) and *big3* / GN-ML-MYC (H) mutants after 1 h treatment with 50 µM BFA. (I to L) Immuno-localization of PEN1 in Col (I), GN-ML-MYC(J), *big3* (K) and *big3* / GN-ML-MYC (L) mutants after 1 h treatment with 50 µM BFA. BFA induced aggregates of apical PIN2 and non-polar PEN1, but not basal PIN1

in the BFA resistant GN-ML-MYC mutants irrespective of *BIG3* mutation. Representative images are shown. Scale bars, 10 µm.

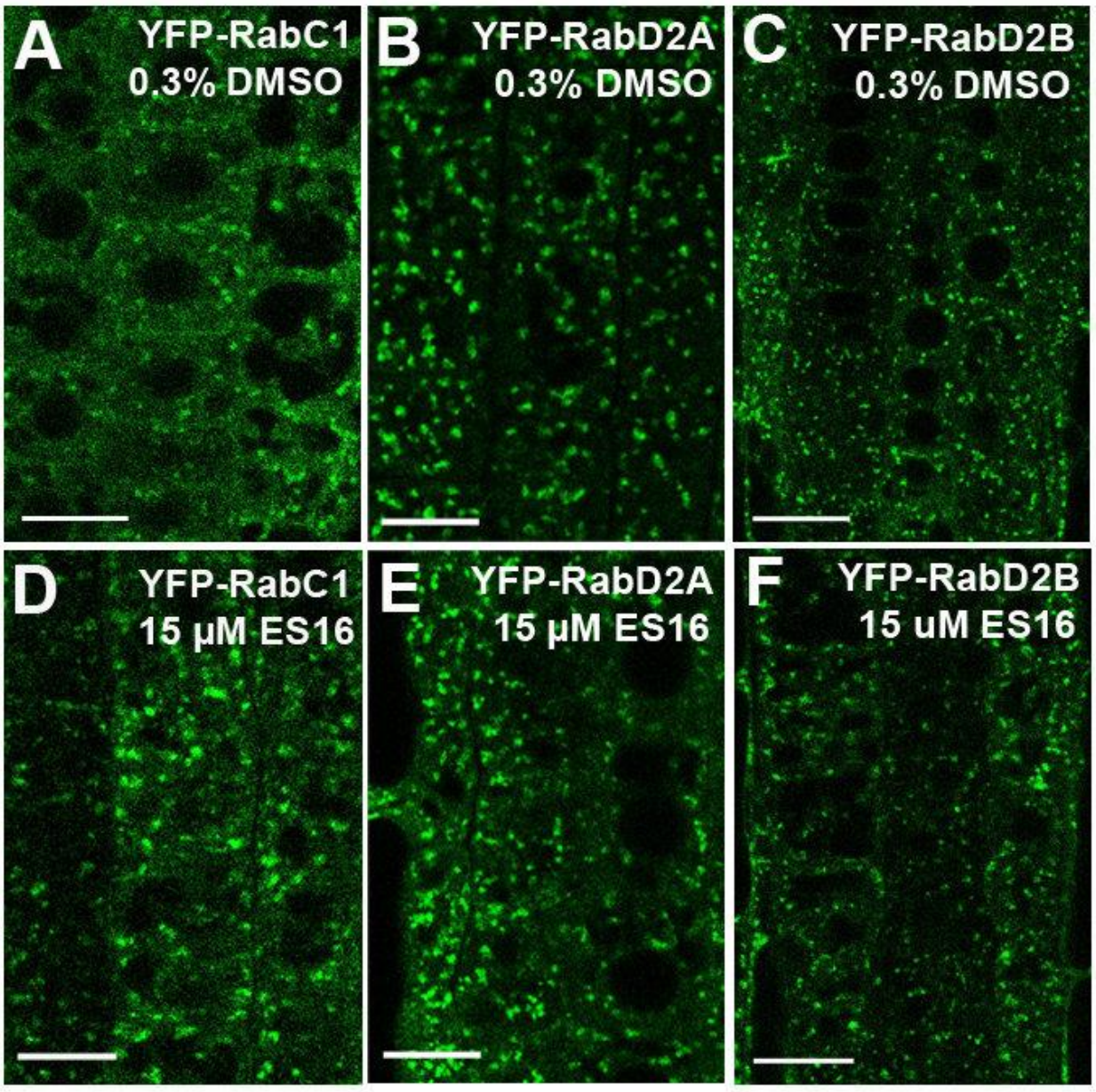

Supplemental Figure 5. ES16 is not a general Rab GTPase inhibitor.

(A to F) ES16 does not perturb the localization of RabC1 (A, D), RabD2A (B, E) or RabD2B (C and F). Images are representative of three repeats. Scale bars, 10 µm.

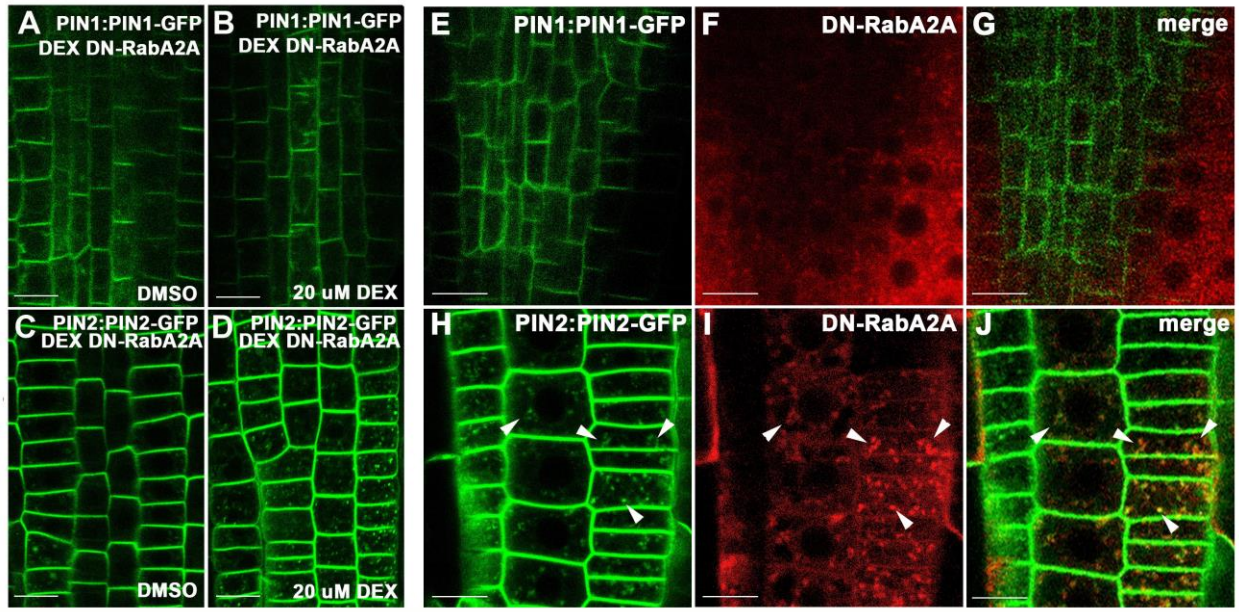

Supplemental Figure 6. Overexpression of DN-RabA2A induces aggregates of PIN2 but not PIN1.

(A and B) 20 µM DEX-induced over-expression of DN-RabA2A does not change the PIN1 protein localization. (C and D) 20 µM DEX-induced over-expression of DN-RabA2A significantly increases PIN2 internalization as visualized by the intracellular vesicles. (E to G) Stable over-expression of DN-RabA2A does not change the PIN1 polarity. (H to J) Stable over-expression of DN-RabA2A results in enhanced PIN2 agglomerations, which are co-localized with the DN-RabA2A vesicles (white arrowheads). Images are representative of three repeats. Scale bars, 10 µm.

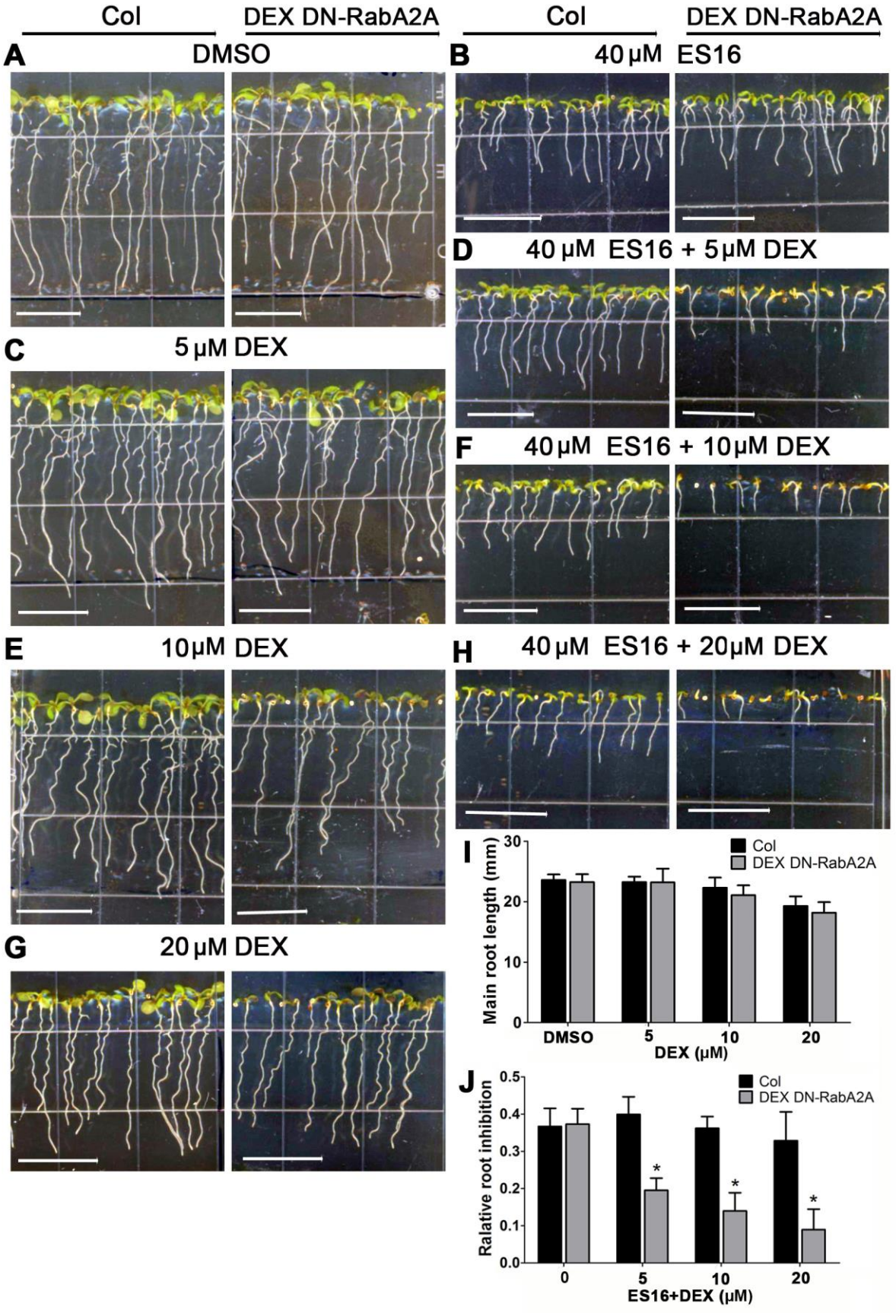
Col
DEX DN-RabA2A
A
DMSO
B
40 μM ES16
C
5 μM DEX
D
40 μM ES16 + 5 μM DEX
E
10 μM DEX
F
40 μM ES16 + 10 μM DEX
G
20 μM DEX
H
40 μM ES16 + 20 μM DEX
I
Main root length (mm)
DMSO
5
10
20
DEX (μM)
J
Ralative root inhibition
ES16+DEX (μM)

Supplemental Figure 7. ES16 shows synergistic effects with RabA2A mutation.

(A, C, E and G) DEX induction did not produce discernable phenotypic defects of DEX DN-RabA2A seedlings. (B, D, F and H) DEX induction resulted in hypersensitivity of DEX DN-RabA2A seedlings on ES16 medium and the response was enhanced with increasing concentration of ES16. (I) Quantification of main root length of seedlings on DMSO medium with different concentrations of DEX as shown in A, C, E and G. (J) Relative root inhibition rate of seedlings on ES16 medium with different concentrations of DEX induction as shown from A to H. Root inhibition was calculated as the ratio of mean root length on ES16 medium to that on DMSO medium with the same concentration of DEX; 80 seedlings per genotype per treatment were selected for measurement. A two-tailed student t-test was used to test the significance. Asterisks represent $p < 0.01$. Bars stand for SD. Scale bars, 1 cm.